From Ribonuclease A toward Bovine Seminal Ribonuclease: A Step by Step Thermodynamic Analysis†

Francesca Catanzano,‡ Giuseppe Graziano,§ Valeria Cafaro,|| Giuseppe D'Alessio,|| Alberto Di Donato,|| and Guido Barone*,‡

Dipartimento di Chimica, Università di Napoli Federico II, Via Mezzocannone 4, 80134 Napoli, Italy, Dipartimento di Chimica, Università di Salerno, Via Salvador Allende, 84081 Baronissi (SA), Italy, and Dipartimento di Chimica Organica e Biologica, Università di Napoli Federico II, Via Mezzocannone 16, 80134 Napoli, Italy

Received June 6, 1997; Revised Manuscript Received September 16, 1997⊗

ABSTRACT: A proline, a leucine, and two cysteine residues, introduced at positions 19, 28, 31, and 32 of bovine pancreatic RNase A, i.e. the positions occupied by these residues in the subunit of bovine seminal RNase, the only dimeric RNase of the pancreatic-type superfamily, transform monomeric RNase A into a dimeric RNase, endowed with the same ability of BS-RNase of swapping its N-terminal segments. The thermodynamic consequences of the progressive introduction of these four residues into RNase A polypeptide chain have been studied by comparing the temperature- and urea-induced denaturation of three mutants of RNase A with that of a stable monomeric derivative of BS-RNase. The denaturation processes proved reversible for all proteins, and well represented by the two-state N ⇔ D transition model. The progressive introduction of the four residues into RNase A led to a gradual shift of the protein stability toward that characteristic of monomeric BS-RNase, which, in turn, is markedly less stable than RNase A with respect to both temperature- and urea-induced denaturation. On the other hand, the thermal stability of a dimeric active mutant of RNase A is found to approach that of wild-type seminal RNase.

Bovine seminal ribonuclease, BS-RNase, is the only dimeric ribonuclease of the pancreatic-type superfamily (D'Alessio et al., 1997). Its two identical subunits, with more than 80% of sequence identity with pancreatic RNase A,[1] are linked by two disulfide bridges between the adjacent half-cystine residues 31 and 32 of both chains. Two dimeric structures have been described for BS-RNase, in equilibrium with each other, the M×M form, in which the subunits exchange their N-terminal segments (Mazzarella et al., 1993), and the M=M form, in which no swapping occurs (Piccoli et al., 1992). Moreover, BS-RNase is endowed with interesting bioactions (D'Alessio et al., 1997), including an antitumor action (Youle & D'Alessio, 1997).

Recently it has been demonstrated (Di Donato et al., 1994, 1995; Kim et al., 1995), that (i) the presence of intersubunit disulfides is a necessary condition to form a stable dimeric RNase; (ii) each of four residues—a Pro, a Leu, and two Cys at positions 19, 28, 31, and 32, respectively—plays a role in determining the exchange of N-terminal segments between subunits. This is a key structural feature for engendering the antitumor action of a dimeric RNase, like BS-RNase. Cys31 and 32 of one subunit form two disulfide bridges with Cys32 and 31, respectively, of the other subunit, giving rise to two covalent cross-links at the interface between monomers (Di Donato & D'Alessio, 1973). Also Leu28 occurs at this interface and its side chain gives rise to a hydrophobic interaction with the side chain of Leu28 of the other subunit. Finally, Pro19 is located in the so-called hinge-peptide constituted by residues 16−22, which connects the N-terminal segment (comprising residues 1−15) to the main body of the molecule (comprising residues 23−124) and is fundamental for the swapping (Mazzarella et al., 1995).

In our effort to study the stability of ribonucleases (Barone et al., 1992b; Catanzano et al., 1996; Graziano et al., 1996b), we investigated the thermodynamic consequences of the introduction into the polypeptide chain of RNase A of the four residues mentioned above, which are the minimal structural requirements for dimerization and swapping. It has been previously found for a monomeric derivative of BS-RNase, MCM-BS-RNase, obtained by selective reduction of the two intersubunit disulfide bridges and carboxymethylation of the free sulfydryl groups (D'Alessio et al., 1975), a marked decrease of thermodynamic stability with respect to both RNase A and BS-RNase (Grandi et al., 1979). We thus investigated, by means of differential scanning calorimetry and circular dichroism, the temperature-induced and urea-induced denaturation of three mutants of RNase A: P-RNase A, PL-RNase A, and MCAM-PLCC-RNase A, a monomeric and carboxyamidomethylated derivative of the

† Work supported by grants from the Italian National Research Council (C. N. R., Rome), and the Italian Ministry for University and Scientific and Technological Research (M. U. R. S. T., Rome).

* Author to whom correspondence should be addressed.

‡ Dipartimento di Chimica, Università di Napoli Federico II.

§ Dipartimento di Chimica, Università di Salerno.

|| Dipartimento di Chimica Organica e Biologica, Università di Napoli Federico II.

⊗ Abstract published in *Advance ACS Abstracts,* November 1, 1997.

[1] Abbreviations: RNase A, bovine pancreatic ribonuclease; P-RNase A, monomeric (A19P) RNase A; PL-RNase A, monomeric (A19P/Q28L) RNase A; PLCC-RNase AA, dimeric (A19P/Q28L/K31C/S32C) RNase A; MCAM-PLCC-RNase A, monomeric [*S*-carboxyamidomethyl-Cys31, *S*-carboxyamidomethyl-Cys32] PLCC-RNase A; BS-RNase, bovine seminal ribonuclease; MCM-BS-RNase, monomeric [*S*-carboxymethyl-Cys31, *S*-carboxymethyl-Cys32] BS-RNase; MCAM-BS-RNase, monomeric [*S*-carboxyamidomethyl-Cys31, *S*-carboxyamidomethyl-Cys32] BS-RNase; M×M, dimeric form of BS-RNase in which the subunits exchange their N-terminal segments; M=M, dimeric form of BS-RNase in which no exchange occurs; DSC, differential scanning calorimetry; CD, circular dichroism; ASA, accessible surface area; NOE, nuclear Overhauser effect; SDS−PAGE, sodium dodecyl sulfate−polyacrylamide gel electrophoresis.

S0006-2960(97)01358-5 CCC: $14.00

dimeric mutant of RNase A, and of MCAM-BS-RNase, a monomeric and carboxyamidomethylated derivative of seminal ribonuclease. The denaturation processes proved reversible and well represented by the two-state N ⇔ D transition model, for all RNases. More interestingly, the progressive introduction of the four residues caused a substantial and stepwise decrease of the thermodynamic stability of RNase A, gradually transforming it into a virtual monomer of BS-RNase.

MATERIALS AND METHODS

Protein Expression and Purification

The cDNAs coding for P-, PL-, and PLCC-RNase A, inserted into the pT7-7 expression vector, were expressed and purified as described previously (Di Donato et al., 1994; 1995). Yields of proteins ranged from 5 to 10 mg per liter of bacterial culture. Carboxyamidomethylated monomers of BS-RNase, and of PLCC-RNase AA, were obtained as described (D'Alessio et al., 1975), through selective cleavage of the intersubunit disulfides, followed by alkylation of the exposed sulfydryl groups with iodoacetamide. RNase A was type XII A of Sigma. Protein purity was checked by SDS−PAGE (Laemmli, 1970). RNase activity on yeast RNA was assayed with the method of Kunitz (1946).

Protein concentration was calculated from spectroscopic measurements by using $A(0.1\%, 278\ \text{nm}) = 0.46$ for BS-RNase; $A(0.1\%, 278\ \text{nm}) = 0.71$ for RNase A, and $A(0.1\%, 278\ \text{nm}) = 0.54$ for MCAM-BS-RNase (Parente et al., 1977). For the three mutants of RNase A we used the same extinction coefficient of the parent enzyme, as the mutations do not alter the content of chromophore groups.

Protein solutions for DSC and CD measurements were exhaustively dialyzed against acetic acid/sodium acetate, pH 5.0, 100 mM at 4 °C, by using Spectra Por MW 6000−8000 membranes. Doubly deionized water was used throughout. The pH of all solutions was determined with a Radiometer pHmeter, model PHM 93, at 25 °C.

Ultrapure urea, purchased from Sigma, was used after recrystallization from ethanol. Urea solutions were prepared fresh daily in buffered solutions containing 100 mM acetate buffer at pH 5.0, and the concentration of the urea stock solution was determined by refractive index measurements (Pace, 1986). Individual samples at different urea concentrations were equilibrated at 4 °C overnight. Each independent sample was placed in the CD instrument and the signal at 222 nm recorded after averaging for 240 s.

Circular Dichroism. CD spectra were recorded with a Jasco J-710 spectropolarimeter. The instrument was calibrated with an aqueous solution of *d*-10-(+)-camphorsulfonic acid at 290 nm (Yang et al., 1986). Molar ellipticity per mean residue ($[\vartheta]$ in deg cm^2 dmol^{-1}), was calculated from the equation: $[\vartheta] = [\vartheta]_{obs}(\text{mrw})/10lC$, where $[\vartheta]_{obs}$ is the ellipticity measured in degrees, mrw is the mean residue molecular weight, 110 Da, C is the protein concentration in g mL^{-1}, and l is the optical path length of the cell in cm. A 0.1 cm path length cell and a protein concentration of about 0.1 mg mL^{-1} were used in the far-UV region. CD spectra were recorded with a time constant of 4 s, a 2 nm band width, and a scan rate of 5 nm min^{-1}. Spectra were signal-averaged over at least five scans, and base line corrected by subtracting a buffer spectrum. Temperature was regulated with a circulating water bath, and monitored with a thermocouple inserted directly into the cell. Thermal unfolding curves were determined in the temperature mode at 222 nm, with a scan rate of 0.5 K min^{-1}. Thermodynamic parameters were calculated by means of a van't Hoff analysis applied to a two-state N ⇔ D transition.

Scanning Calorimetry. Calorimetric measurements were carried out on a second-generation Setaram Micro-DSC apparatus, interfaced with a data translation A/D board for automatic data accumulation. A scan rate of 0.5 K min^{-1} was chosen for the present study. All data analyses were accomplished with software developed in our laboratory (Barone et al., 1992a). Raw data were converted to an apparent molar heat capacity by correcting for the instrument calibration curve and the buffer−buffer scanning curve, and by dividing each data point by the scan rate and the protein molarity in the sample cell. The excess heat capacity function $\langle \Delta C_p \rangle$ was obtained after base line subtraction, assuming that the base line is given by the linear temperature dependence of native state heat capacity (Freire & Biltonen, 1978). The calorimetric enthalpy $\Delta_d H(T_d)$ was determined by direct integration of the area under the curve, and the van't Hoff enthalpy was calculated with the standard formula (Privalov, 1979):

$$\Delta_d H_{vH}(T_d) = 4RT_d^2[\langle \Delta C_p(T_d) \rangle / \Delta_d H(T_d)] \qquad (1)$$

where T_d is the denaturation temperature and corresponds to the maximum of the DSC peak, $\langle \Delta C_p(T_d) \rangle$ is the value of the excess heat capacity function at T_d, and R is the gas constant. The closeness to 1 of the cooperative unit, defined as the calorimetric to van't Hoff enthalpy ratio, $\text{CU} \equiv \Delta_d H(T_d)/\Delta_d H_{vH}(T_d)$, is a necessary condition to state that the denaturation is a two-state transition.

RESULTS AND DISCUSSION

Temperature-Induced Denaturation at pH 5.0

DSC measurements were performed at pH 5.0, 100 mM acetate buffer, to compare the thermal stability of RNase A with that of the mutant proteins P-RNase A, PL-RNase A, MCAM-PLCC-RNase A, and with that of MCAM-BS-RNase. The results are reported in Table 1, whereas the DSC curves are shown in Figure 1. The temperature-induced denaturation of the proteins is well represented by the two-state N ⇔ D transition model, as indicated by the closeness to 1 of the cooperative unit values (see Table 1). All transitions proved reversible, according to the reheating criterion, and not influenced by protein concentration (in the range 1.4−3.0 mg mL^{-1}), which further validates the two-state N ⇔ D model.

We also performed CD measurements at 222 nm as a function of temperature at pH 5.0, 100 mM acetate buffer. Also these thermal denaturation profiles proved reversible, according to the reheating criterion, and were analyzed by the van't Hoff procedure, assuming valid the two-state N ⇔ D model. The denaturation parameters derived from CD transition curves agree with those directly obtained from DSC scans (see Table 1).

The single substitution A19P decreases the denaturation temperature by 1.7 °C, as T_d is lowered from 61.3 °C, the value for RNase A, to 59.6 °C for P-RNase A. This result seems to contrast with the prediction (Nemethy et al., 1966;

Table 1: Thermodynamic Parameters of the Temperature-Induced Denaturation of the Five Ribonucleases, Obtained from Both DSC and CD Measurements, at pH 5.0, 100 mM Acetate Buffer[a]

		T_d (°C)	$\Delta_dH(T_d)$ (kJ mol^{-1})	$\Delta_dS(T_d)$ (kJ K^{-1} mol^{-1})	Δ_dC_p (kJ K^{-1} mol^{-1})	CU
RNase A	DSC	61.3	465 ± 13	1.39 ± 0.04	5.5 ± 0.6	1.01
	CD	61.2	460 ± 14	1.38 ± 0.05	−	−
P-RNase A	DSC	59.6	415 ± 13	1.25 ± 0.04	5.2 ± 0.6	1.03
	CD	59.4	415 ± 15	1.25 ± 0.05	−	−
PL-RNase A	DSC	59.0	410 ± 12	1.23 ± 0.04	5.0 ± 0.6	0.99
	CD	58.8	400 ± 14	1.20 ± 0.05	−	−
MCAM-PLCC-RNase A	DSC	56.4	390 ± 12	1.18 ± 0.04	4.8 ± 0.5	0.99
	CD	56.1	385 ± 15	1.17 ± 0.05	−	−
MCAM-BS-RNase	DSC	55.2	380 ± 12	1.16 ± 0.04	4.7 ± 0.5	0.97
	CD	55.1	375 ± 15	1.14 ± 0.05	−	−

[a] CU refers to cooperative unit and is the ratio of the calorimetric to van't Hoff enthalpy, evaluated at the denaturation temperature. *Note*. Each figure is the mean value of four measurements. The error in T_d does not exceed 0.2 °C. Reported errors for $\Delta_dH(T_d)$ and Δ_dC_p are the standard deviations of the mean from the multiple determinations. Errors for $\Delta_dS(T_d)$ are calculated by propagating the errors for $\Delta_dH(T_d)$ and T_d.

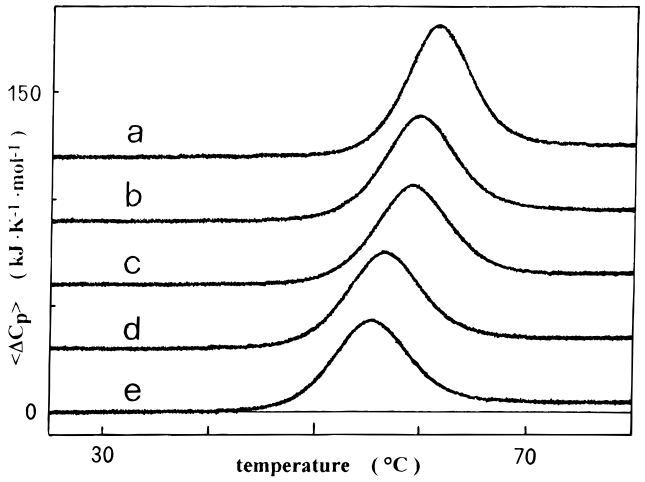

FIGURE 1: DSC profiles at pH 5.0, 100 mM acetate buffer, of RNase A (curve a); P-RNase A (curve b); PL-RNase A (curve c); MCAM-PLCC-RNase A (curve d); MCAM-BS-RNase (curve e). The curves have been shifted along the *y*-axis for ease of presentation.

Matthews et al., 1987) that the introduction of a proline residue should cause an entropic stabilization of the native structure due to the lower conformational freedom of the denatured state. However, theoretical calculations (Mazzarella et al., 1995), performed by means of the ECEPP force-field (Nemethy et al., 1992), applied to the hinge-peptide 16−22 of RNase A with Pro substituting for Ala19, showed that Pro19 assumes a trans conformation determining a shift toward the exterior of the molecule of the hinge-peptide. This substitution beyond causing a decrease of the conformational freedom in the denatured state, increases the local flexibility of the polypeptide chain in the native state, by weakening the noncovalent interactions with the main body of the molecule. The lowest energy structure theoretically predicted was found to possess 38 kJ mol^{-1} of nonbonded energy in excess with respect to RNase A. Our results are in agreement with this prediction, as both the denaturation enthalpy and entropy changes decrease upon the A19P substitution (see Table 1). Therefore, the lower thermal stability of P-RNase A with respect to the native enzyme is due to the prevalence of the destabilizing enthalpic factor over the stabilizing entropic one.

For PL-RNase A, both the denaturation temperature and the enthalpy change show a further decrease, being T_d = 59.0 °C and $\Delta_dH(T_d)$ = 410 kJ mol^{-1}. Such a decrease is likely due to the exposure of residue 28 to the solvent, and to the substitution of a hydrophobic residue as leucine for a polar one, such as glutamine. A marked decrease of thermal stability with respect to the native enzyme occurs in the case of MCAM-PLCC-RNase A, that shows T_d = 56.4 °C and $\Delta_dH(T_d)$ = 390 kJ mol^{-1}. Residues 31 and 32 are located in an α-helix segment in both pancreatic (Wlodawer et al., 1988), and seminal RNases (Mazzarella et al., 1993), so that thermal stability changes could be rationalized according to the helix propensities of the mutated residues. It results that Cys has a lower helix propensity than both Lys and Ser (Chakrabartty & Baldwin, 1995). Therefore, the decreased stability of MCAM-PLCC-RNase A with respect to PL-RNase A matches the expectation from the rank order of helix propensities.

For MCAM-BS-RNase T_d = 55.2 °C and $\Delta_dH(T_d)$ = 380 kJ mol^{-1}, close to those measured for MCAM-PLCC-RNase A. This indicates that the cumulative effects of the four mutations are responsible of the marked destabilization of MCAM-PLCC-RNase A with respect to RNase A.

The Δ_dC_p value of RNase A was determined by linear regression of the $\Delta_dH(T_d)$ vs T_d plot in the pH range 3.0−6.0 (data not shown), whereas the Δ_dC_p values for the other four proteins were determined from several individual DSC scans at pH 5.0. It should be noted the qualitative lowering trend in the mean values of Δ_dC_p, going from RNase A to MCAM-BS-RNase (see Table 1). On the basis of models developed to calculate Δ_dC_p (Murphy & Freire, 1992; Makhatadze & Privalov, 1995; Graziano et al., 1996a), this trend could be due to a greater exposure to water of nonpolar groups in the native conformation of mutants and MCAM-BS-RNase, assuming that the denatured state is almost identical for the proteins investigated.

A thermodynamic analysis of the relative influence of the introduction of mutations into a polypeptide chain requires the evaluation of Δ_dH and Δ_dS at the same temperature for the different mutant proteins (Vogl et al., 1995). To this purpose, we used only the values from DSC measurements because Δ_dC_p has to be accurately known. We selected as reference the denaturation temperature of MCAM-BS-RNase, T_d = 55.2 °C, to minimize errors associated with the extrapolation procedure. For a two-state transition, assuming Δ_dC_p as temperature-independent, the denaturation enthalpy and entropy can be calculated according to the following equations (Privalov, 1979):

$$\Delta_dH(T) = \Delta_dH(T_d) + \Delta_dC_p(T - T_d) \quad (2)$$

$$\Delta_dS(T) = [\Delta_dH(T_d)/T_d] + \Delta_dC_p \ln(T/T_d) \quad (3)$$

Table 2: Comparison between the Denaturation Enthalpy and Entropy Changes of the Five Ribonucleases Evaluated at the Same Reference Temperature, 55.2 °C, Corresponding to the Denaturation Temperature of MCAM-BS-RNase at pH 5.0, 100 mM Acetate Buffer[a]

	Δ_dH(55.2 °C) (kJ mol^{-1})	Δ_dS(55.2 °C) (kJ K^{-1} mol^{-1})
RNase A	431 ± 13	1.29 ± 0.04
P-RNase A	392 ± 13	1.18 ± 0.04
PL-RNase A	391 ± 12	1.18 ± 0.04
MCAM-PLCC-RNase A	384 ± 12	1.17 ± 0.04
MCAM-BS-RNase	380 ± 12	1.16 ± 0.04

[a] Errors for Δ_dH(55.2 °C) and Δ_dS(55.2 °C) are propagated using formulas derived according to Bevington and Robinson (1992).

The assumption of the temperature-independence of Δ_dC_p is justified in this case by the narrow temperature range involved. The resulting quantities, reported in Table 2, confirm that statistically significant decreases of both Δ_dH(55.2 °C) and Δ_dS(55.2 °C) are due to the introduction of proline at position 19. The enthalpy difference between RNase A and P-RNase A amounts to 39 ± 19 kJ mol^{-1} at 55.2 °C, in line with the theoretical calculations (Mazzarella et al., 1995). A comparison of RNase A with MCAM-BS-RNase leads to values of $\Delta\Delta_dH$(55.2 °C) = 51 ± 18 kJ mol^{-1} and $\Delta\Delta_dS$(55.2 °C) = 130 ± 60 J K^{-1} mol^{-1}. Thus, from a thermodynamic point of view, it seems that the structure of the monomeric form of BS-RNase is less stable than that of RNase A, with the marked decrease of thermal stability due to enthalpic factors, only partially counterbalanced by entropic factors.

This interpretation is supported also by the 2-D and 3-D ^{1}H-NMR data (D'Ursi et al., 1995), which led to the determination of the secondary structure of MCM-BS-RNase, and to an initial model of its tertiary structure with a folding pattern very similar to that of RNase A. In the model some differences remain in the chain segments that contain multiple amino acid substitutions with respect to RNase A. In particular, a trans conformation was assigned to Pro19, which causes a shift toward the exterior of the protein, not only of the hinge-peptide, but of the entire N-terminal segment. It was also stressed that the pattern of NOE signals between the residues of the N-terminal segment and those of the main body of the molecule, indicates that the two parts do not interact as strongly as in RNase A.

The structural evidence from NMR data collected on monomeric BS-RNase (D'Ursi et al., 1995), and the theoretical analysis of the RNase A mutant with Pro at position 19 (Mazzarella et al., 1995), are in agreement with our data on the substantial difference in thermal stability between RNase A and MCAM-BS-RNase, and confirm the key role played by Pro19 in weakening the interactions between the N-terminal segment and the main body of BS-RNase. Furthermore, the structural information justify the interpretation that the stepwise decrease in thermal stability associated with the four mutations is mainly due to structural alterations in the native state of mutant proteins with respect to that of RNase A.

Urea-Induced Denaturation at pH 5.0

Circular dichroism at 222 nm was used to monitor the urea-induced denaturation at 25 °C, pH 5.0, 100 mM acetate buffer, to compare the stability of the five proteins. Denaturation processes were reversible for all proteins under the experimental conditions used. We assumed valid the two-state N ↔ D model for the urea-induced denaturation and calculated the standard Gibbs energy of denaturation Δ_dG according to the equation

$$\Delta_dG = -RT \ln K_d = -RT \ln[([\vartheta] - [\vartheta]_N)/([\vartheta]_D - [\vartheta])] \quad (4)$$

where K_d is the equilibrium constant, $[\vartheta]$ is the observed value of molar ellipticity, and $[\vartheta]_N$ and $[\vartheta]_D$ are the values characteristic of the native and denatured states, respectively. A least-squares analysis of data in the pre- and post-transition regions makes it possible to extrapolate $[\vartheta]_N$ and $[\vartheta]_D$ in the transition region. Δ_dG, calculated with eq 4, resulted a linear function of urea concentration and a least-squares regression was used to fit the data to the equation

$$\Delta_dG = \Delta_dG(H_2O) - m[\text{urea}] \quad (5)$$

where $\Delta_dG(H_2O)$ is the value of Δ_dG in the absence of urea and m is a measure of the dependence of Δ_dG on urea concentration. Clearly, $\Delta_dG(H_2O) = m[\text{urea}]_{1/2}$, where $[\text{urea}]_{1/2}$ is a measure of the midpoint of the denaturation region. Santoro and Bolen (1988) pointed out that such application of the linear extrapolation model to analyze urea unfolding curves underestimates the uncertainty in the parameters calculated, because no error is assumed for the pre- and post-transition base lines. In our case, however, the method may be acceptable because the proteins are homologous and we are only interested in a comparison among them.

Table 3: Thermodynamic Parameters of the Urea-Induced Denaturation at 25 °C, pH 5.0, 100 mM Acetate Buffer, of the Five Ribonucleases[a]

	$[\text{urea}]_{1/2}$ (M)	m (kJ mol^{-1} M^{-1})	$\Delta_dG(H_2O)$ (kJ mol^{-1})	Δ_dG(25 °C) (kJ mol^{-1})
RNase A	5.2	7.1 ± 0.3	36.9 ± 2.5	39.2
P-RNase A	4.9	6.6 ± 0.4	32.3 ± 2.6	33.5
PL-RNase A	4.8	6.5 ± 0.4	31.7 ± 2.8	33.0
MCAM-PLCC-RNase A	4.5	6.2 ± 0.5	27.9 ± 3.0	29.7
MCAM-BS-RNase	4.3	6.2 ± 0.4	26.7 ± 2.7	28.2

[a] The values reported are the results of linear least-squares regressions of Δ_dG vs [urea] plots; $[\text{urea}]_{1/2} = [\Delta_dG(H_2O)/m]$ is the midpoint of the urea unfolding curve. The values of Δ_dG(25 °C) are calculated by eq 6, with the parameters determined by DSC measurements. *Note*. Reported errors are the standard deviations of linear regressions.

The values of the parameters m, $\Delta_dG(H_2O)$, and $[\text{urea}]_{1/2}$, derived from the linear regressions of experimental data to eq 5, are reported in Table 3. Urea-unfolding curves are shown in Figure 2, where f_D represents the fraction of denatured molecules, and the solid lines have been calculated with the parameter values determined by linear regressions. It is evident that the stepwise introduction of the four residues into the polypeptide chain of RNase A causes a gradual decrease in stability, as $[\text{urea}]_{1/2}$ lowers from 5.2 M for RNase A to 4.5 M for MCAM-PLCC-RNase A, close to the value determined for MCAM-BS-RNase, 4.3 M. In addition, the values of $\Delta_dG(H_2O)$ decrease from 36.9 kJ mol^{-1} for RNase A to 26.7 kJ mol^{-1} for MCAM-BS-RNase. These values agree, within experimental errors, with those calculated at 25 °C according to the equation

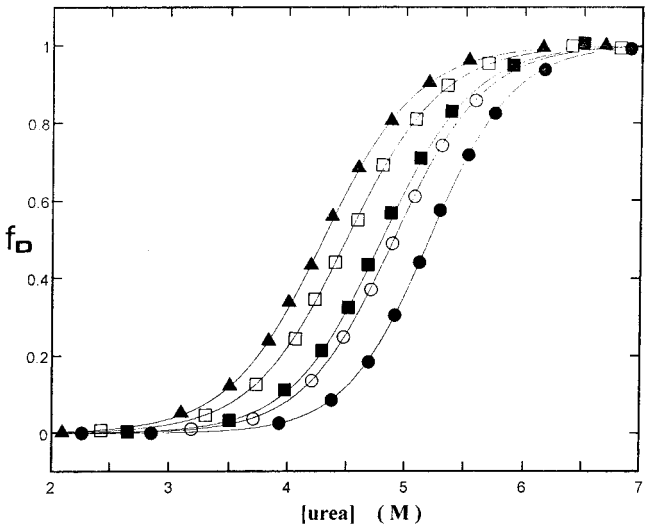

FIGURE 2: Urea unfolding curves determined by monitoring the CD signal at 222 nm, pH 5.0, 100 mM acetate buffer, $T = 25$ °C: (●) RNase A; (○) P-RNase A; (■) PL-RNase A; (□) MCAM-PLCC-RNase A; (▲) MCAM-BS-RNase. The solid lines are based on the parameters derived from linear least-squares regressions of the experimental data.

$$\Delta_d G(T) = \Delta_d H(T_d)[1 - (T/T_d)] + \Delta_d C_p[T - T_d - T\ln(T/T_d)] \quad (6)$$

using the values determined by DSC measurements and considering $\Delta_d C_p$ to be temperature-independent (see Table 3).

Temperature-Induced Denaturation of Dimeric Forms at pH 5.0

It has been reported that the denaturation temperature of dimeric BS-RNase is similar to that of RNase A, whereas a monomeric derivative of BS-RNase, i.e. MCM-BS-RNase, is markedly less stable (Grandi et al., 1979). This latter datum is perfectly superimposable to those reported in the present study on the reduced thermal stability of MCAM-BS-RNase with respect to RNase A. However, it prompted the question of whether the mutants of RNase A under investigation, whose thermodynamic parameters continously shift toward those characteristic of the monomeric derivative of BS-RNase, would become similar to BS-RNase upon dimerization.

We thus prepared dimeric PLCC-RNase AA and performed DSC measurements at pH 5.0, 100 mM acetate buffer, using, as a reference protein, dimeric bovine seminal ribonuclease. In both cases (see Figure 3), DSC profiles proved reversible, and showed a denaturation temperature of about 61.6 °C and an enthalpy change around 700 kJ mol^{-1}, even though the process is not well represented by the two-state N ⇔ D transition model, as indicated by the asymmetry of the peak. It should be underlined that both proteins, BS-RNase and dimeric PLCC-RNase AA, are a mixture of the two quaternary conformations, M×M and M=M, in a molar ratio 2/1. Thus, it is not possible to further analyze such DSC curves because they represent the behavior of a mixture of two conformations in equilibrium with each other, and probably with different stability. At any rate, the DSC profiles strongly suggest that dimeric PLCC-RNase AA has a thermal stability very similar to that of BS-RNase. Thus, our data confirm that the four amino acid replacements

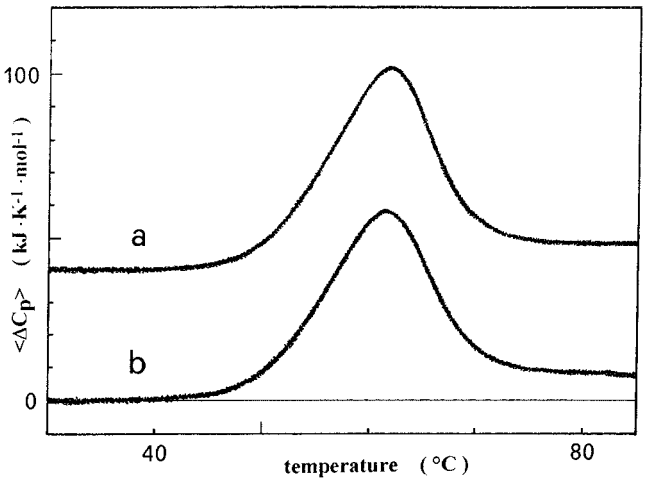

FIGURE 3: DSC profiles at pH 5.0, 100 mM acetate buffer, of dimeric BS-RNase (curve a), and dimeric PLCC-RNase AA (curve b). Both the proteins are a mixture of M×M and M=M quaternary structures. The curves have been shifted along the *y*-axis for ease of presentation.

are the structural determinants which convert monomeric RNase A into a dimeric molecule similar, if not identical, to BS-RNase (Di Donato et al., 1995), hence with a similar thermal stability.

The increase in denaturation temperature found in dimeric RNases with respect to their monomeric forms can be rationalized on structural grounds. The two intersubunit disulfide bridges, pairing Cys31 and 32 of one subunit with Cys32 and 31, respectively, of the other subunit, should stabilize the protein, primarily by reducing the conformational entropy of the denatured state relative to the native one.

The findings reported above also may bear an evolutionary significance, as they confirm that the evolutionary lines leading to bovine pancreatic and seminal RNase are distinct, with distant immediate ancestors (Beintema et al., 1997). The insertion of residues such as Cys31 and 32, Pro19, and Leu28 in (monomeric) ancestors of seminal RNase rendered monomeric RNases less stable, thus unavoidably leading to the only dimeric, stable RNase.

REFERENCES

Barone, G., Del Vecchio, P., Fessas, D., Giancola, C., & Graziano, G. (1992a) *J. Thermal Anal. 38*, 2779−2790.

Barone, G., Del Vecchio, P., Fessas, D., Giancola, C., Graziano, G, Pucci, P., Ruoppolo, M., & Riccio, A. (1992b) *J. Thermal Anal. 38*, 2791−2802.

Beintema, J. J., Breukelman, H. J., Carsana, A., & Furia, A. (1997) in *Ribonucleases: Structures and Function* (D'Alessio, G., & Riordan, J. F., Eds.) pp 245−269, Academic Press, New York.

Bevington, P. R., & Robinson, D. K. (1992) *Data Reduction and Error Analysis for the Physical Sciences*, McGraw-Hill, New York.

Catanzano, F., Giancola, C., Graziano, G., & Barone, G. (1996) *Biochemistry 35*, 13378−13385.

Chakrabartty, A., & Baldwin, R. L. (1995) *Adv. Protein Chem. 46*, 141−176.

D'Alessio, G., Malorni, M. G., & Parente, A. (1975) *Biochemistry 14*, 1116−1122.

D'Alessio, G., Di Donato, A., Mazzarella, L., & Piccoli, R. (1997) in *Ribonucleases: Structures and Function* (D'Alessio, G., & Riordan, J. F., Eds.) pp 383−423, Academic Press, New York.

Di Donato, A., & D'Alessio, G. (1973) *Biochem. Biophys. Res. Commun. 55*, 919−928.

Di Donato, A., Cafaro, V., & D'Alessio, G. (1994) *J. Biol. Chem. 269*, 17394−17396.
Di Donato, A., Cafaro, V., Romeo, I., & D'Alessio, G. (1995) *Protein Sci. 4*, 1470−1477.
D'Ursi, A., Oschkinat, H., Cieslar, C., Picone, D., D'Alessio, G., Amodeo, P., & Temussi, P. A. (1995) *Eur. J. Biochem. 229*, 494−502.
Freire, E., & Biltonen, R. L. (1978) *Biopolymers 17*, 463−479.
Grandi, C., D'Alessio, G., & Fontana, A. (1979) *Biochemistry 18*, 3413−3420.
Graziano, G., Catanzano, F., Del Vecchio, P., Giancola, C., & Barone, G. (1996a) *Gazz. Chim. Ital. 126*, 559−567.
Graziano, G., Catanzano, F., Giancola, C., & Barone, G. (1996b) *Biochemistry 35*, 13386−13392.
Kim, J. S., Soucek, J., Matousek, J., & Raines, R. T. (1995) *J. Biol. Chem. 270*, 10525−10530.
Kunitz, M. (1946) *J. Biol. Chem. 164*, 563−568.
Laemmli, U. (1970) *Nature 227*, 680−685.
Makhatadze, G. I., & Privalov, P. L. (1995) *Adv. Protein Chem. 47*, 307−425.
Matthews, B. W., Nicholson, H., & Becktel, W. J. (1987) *Proc. Natl. Acad. Sci. U.S.A. 84*, 6663−6667.
Mazzarella, L., Capasso, S., Demasi, D., Di Lorenzo, G., Mattia, C. A., & Zagari, A. (1993) *Acta Crystallogr. D49*, 389−402.
Mazzarella, L., Vitagliano, L., & Zagari, A. (1995) *Proc. Natl. Acad. Sci. U.S.A. 92*, 3799−3803.
Murphy, K. P., & Freire, E. (1992) *Adv. Protein Chem. 43*, 313−361.
Nemethy, G., Leach, S. J., & Scheraga, H. A. (1966) *J. Phys. Chem. 70*, 998−1004.
Nemethy, G., Gibson, K. D., Palmer, K. A., Yoon, C. N., Paterlini, M. G., Zagari, A., Rumsey, S., & Scheraga, H. A. (1992) *J. Phys.Chem. 96*, 6472−6484.
Pace, C. N. (1986) *Methods Enzymol. 131*, 266−280.
Parente, A., Albanesi, D., Garzillo, A. M., & D'Alessio, G. (1977) *Ital. J. Biochem. 26*, 451−466.
Piccoli, R., Tamburrini, M., Piccialli, G., Di Donato, A., Parente, A., & D'Alessio, G. (1992) *Proc. Natl. Acad. Sci. U.S.A. 89*, 1870−1874.
Privalov, P. L. (1979) *Adv. Protein Chem. 33*, 167−241.
Santoro, M. M., & Bolen, W. (1988) *Biochemistry 27*, 8063−8068.
Vogl, T., Brengelmann, R., Hinz, H. J., Scharf, M., Lotzbeyer, M., & Engels, J. W. (1995) *J. Mol. Biol. 254*, 481−486.
Wlodawer, A., Svensson, L. A., Sjolin, L., & Gilliland, G. L. (1988) *Biochemistry 27*, 2705−2717.
Yang, J. T., Wu, C. S. C., & Martinez, H. N. (1986) *Methods Enzymol. 130*, 208−269.
Youle, R. J., & D'Alessio, G. (1997) in *Ribonucleases: Structures and Function* (D'Alessio, G., & Riordan, J. F., Eds.) pp 491−514, Academic Press, New York.

BI971358J